

## Intersubband relaxation time for $\text{In}_x\text{Ga}_{1-x}\text{As}/\text{AlAs}$ quantum wells with large transition energy

G. Ghisloti,<sup>a)</sup> E. Riedo,<sup>b)</sup> D. Ielmini,<sup>c)</sup> and M. Martinelli  
CoreCom, via Ampere 30, 20131 Milano, Italy

(Received 19 July 1999; accepted for publication 13 October 1999)

Intersubband relaxation time for  $\text{In}_x\text{Ga}_{1-x}\text{As}/\text{AlAs}$  multiple quantum wells presenting a large transition energy (680 meV) is measured by means of pump and probe experiments. Differential transmission decays in about 10 ps. The possible influence of intrasubband relaxation and  $\Gamma-X$  coupling on intersubband decay is discussed. © 1999 American Institute of Physics.  
[S0003-6951(99)01749-0]

Mechanisms responsible for intersubband (ISB) relaxation in quantum wells (QWs) are very important both from a fundamental physics perspective and for device applications. ISB transitions are involved in several optoelectronic devices such as quantum cascade lasers,<sup>1</sup> infrared detectors,<sup>2</sup> and optical modulators.<sup>3</sup> Recent measurements performed in QWs determined an ISB relaxation time in the range of 1–10 ps when the well is narrow enough to make ISB energy larger than the longitudinal optical phonon.<sup>4–6</sup> In large QWs (24 nm), relaxation times of the order of 100 ps were attributed to interaction with acoustic phonons.<sup>7</sup> Typical wavelengths for all the above-mentioned ISB transitions are longer than 4  $\mu\text{m}$ .

In order to take advantage of the fast relaxation time for applications in the optical fiber transmission window around 1.55  $\mu\text{m}$ , ISB transition energy has to be increased. The system  $\text{InGaAs}/\text{AlAs}$  thanks to the large conduction-band offset, allows a large tunability of the ISB energy up to the near-infrared spectral region. Smet *et al.*<sup>8</sup> presented results on  $\text{InGaAs}/\text{AlAs}$  QW showing ISB absorption at 0.8 eV (corresponding to 1.55  $\mu\text{m}$  wavelength) which represents the highest ISB energy reached so far. Asano *et al.*<sup>9,10</sup> realized  $\text{In}_x\text{Ga}_{1-x}\text{As}/\text{AlAs}$  ( $0.2 < x < 0.4$ ) MQWs have a band offset of 1.1–1.3 eV. They proposed to use ISB absorption to optically modulate a light beam resonant with the interband transition. To implement this ultrafast modulator configuration, it is necessary to have similar wavelengths for both interband and intersubband transitions, and therefore  $\text{InGaAs}$  QWs are just a few monolayer (ML) thick with high In content. However, in such a case, quantum confinement effects may raise the  $\Gamma$  conduction-band state of the  $\text{InGaAs}$  well above the conduction-band state ( $X$  state) of the  $\text{AlAs}$  barrier, leading to an indirect band-gap configuration. Jancu *et al.*<sup>11</sup> calculated that one can achieve similar interband and intersubband transition energies before the crossover from type I to type II quantum well occurs. However, for  $\text{In}_x\text{Ga}_{1-x}\text{As}$  (6 ML)/ $\text{AlAs}$  QWs, ISB absorption is already inhibited, due to

electron transfer to the  $X$ -like barrier state. Experimental evidence for the  $\Gamma-X$  transfer in heterostructures having  $\text{AlAs}$  barriers has been reported already.<sup>12,13</sup> When transfer to indirect states occurs, carrier dynamics is controlled by the slow relaxation to the  $\Gamma$  state. This effect can negatively affect the overall relaxation time.

In this work, we present time-resolved pump-probe experiment in  $\text{In}_{0.3}\text{Ga}_{0.7}\text{As}/\text{AlAs}$  MQWs to determine ISB relaxation time. Relaxation time for  $\text{InGaAs}/\text{AlAs}$  QWs having ISB spacing of 0.5 eV has been measured by Asano *et al.*<sup>14</sup> However, in this structure,  $\Gamma-X$  transfer is not effective, hence its influence on the overall ISB relaxation cannot be investigated. Structure investigated in the present work, works at about 0.68 eV, i.e., very close to the regime where  $\Gamma-X$  transfer strongly affects carrier relaxation dynamics. Although relaxation time for ISB transitions in the range of 0.6–0.7 eV has been estimated of the order of 2–9 ps,<sup>9</sup> no direct experimental evidence has been given so far.

Samples were grown by molecular-beam epitaxy on  $\text{GaAs}(001)$  substrates and consisted of a 0.5  $\mu\text{m}$   $\text{GaAs}$  buffer layer grown at 540 °C followed by 30 (8 ML thick)  $\text{In}_{0.3}\text{Ga}_{0.7}\text{As}$  QWs grown at 540 °C with 30 s growth interruption at each interface separated by an 108-Å-thick (36 ML)  $\text{AlAs}$  barrier. A 10-nm-thick  $\text{GaAs}$  cap layer grown at the same temperature concluded the growth.  $\text{In}_{0.3}\text{Ga}_{0.7}\text{As}$  QWs were Si doped to  $1.4 \times 10^{19} \text{cm}^{-3}$ . High-resolution electron-microscopy images were used to confirm well and barrier widths.

Transmission and degenerate pump and probe experiments were performed using the multipass waveguide structure shown in the insert of Fig. 1. Samples were 200  $\mu\text{m}$  thick and 6 mm long. With this configuration light beam propagates across the MQW structure about 30 times. Incident light was transverse magnetic (TM) polarized in order to satisfy selection rules for ISB absorption. Pump and probe beams were obtained from a Ti:sapphire-pumped parametric amplifier delivering 120 fs pulses in the 1.4–2  $\mu\text{m}$  spectral region. Both pump and probe beams were at 1830 nm and TM polarized with respect to the incidence plane. Pump beam was focused on a spot size of about 100  $\mu\text{m}$ . Transmitted probe beam was detected using a PbS detector and standard lock-in detection. Care was taken to reduce residual pump transmission. Pump and probe beams were chopped at

<sup>a)</sup>Present address: Photonic Components, Pirelli Optical Systems, viale Sarca 222, 20126 Milano; electronic mail: giorgio.ghisloti@pirelli.com

<sup>b)</sup>Present address: ESRF, Avenue des Martyrs BP 220 F-38047 Grenoble, France.

<sup>c)</sup>Present address: Dipartimento di Ingegneria Nucleare, Politecnico di Milano, via Ponzio 34, 20133 Milano.

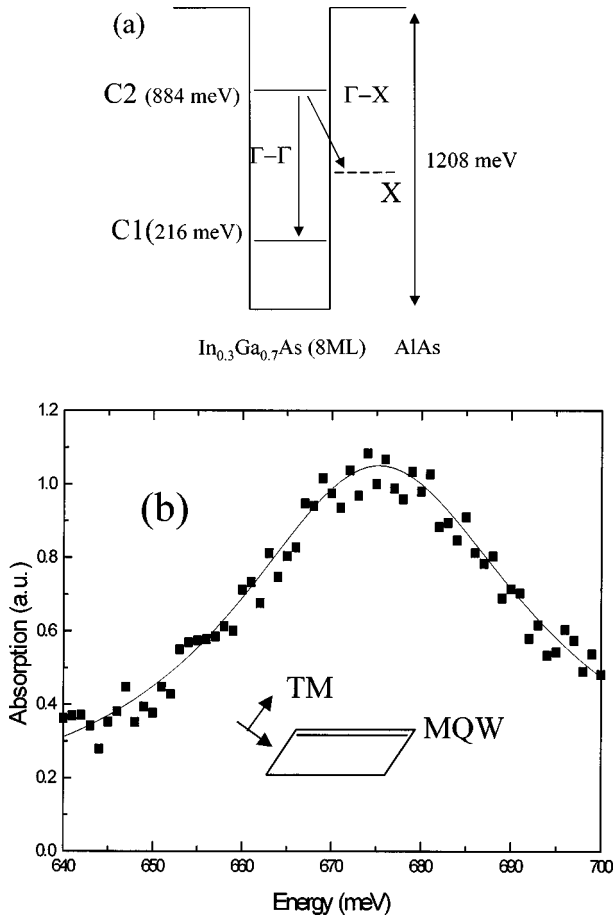


FIG. 1. (a) Conduction-band energy levels calculated as in Ref. 15 and (b) absorption curve. The full line in (b) was calculated according to formula (1). Insert in (b) shows the multipass waveguide configuration adopted for the transmission measurements.

different frequencies in order to extract differential transmission.

Spectral dependence of the room temperature ISB transmission shows a peak at about 680 meV, which is in good agreement with the calculated energy spacing between the two conduction-band states (labeled C1 and C2 in Fig. 1). Energy levels C1 and C2 in Fig. 1(a) and corresponding wave functions were calculated using the method discussed in Ref. 15, while material parameters were taken from Refs. 15 and 16. From the calculated wave functions for the conduction band states  $|1\rangle$  and  $|2\rangle$ , we obtained a dipole matrix element  $M_{12} = \langle 1|z|2\rangle = 6.8 \text{ \AA}$ . These results are in good agreement with tight-binding calculations reported for the same structure.<sup>11</sup> Using the density matrix method, ISB absorption can be derived as<sup>17</sup>

$$\alpha(\omega) = \omega \sqrt{\frac{\mu}{\epsilon}} M_{12}^2 \frac{m_w k_B T}{2L\pi\hbar^2} \ln \frac{1 + \exp[(E_F - E_1)/k_B T]}{1 + \exp[(E_F - E_2)/k_B T]} \times \frac{\hbar\gamma}{(E_2 - E_1 - \hbar\omega)^2 + (\hbar\gamma)^2}, \quad (1)$$

where  $\gamma$  is the dephasing rate,  $\mu$  and  $\epsilon$  are the well permeability and dielectric function,  $L$  is the well width, and  $m_w$  is the electron mass defined as in Ref. 17. Calculated ISB absorption is reported as full line in Fig. 1.

Integrated absorption (i.e., integral of 1 with respect to  $\omega$ ) changes with pump beam intensity according to<sup>17</sup>

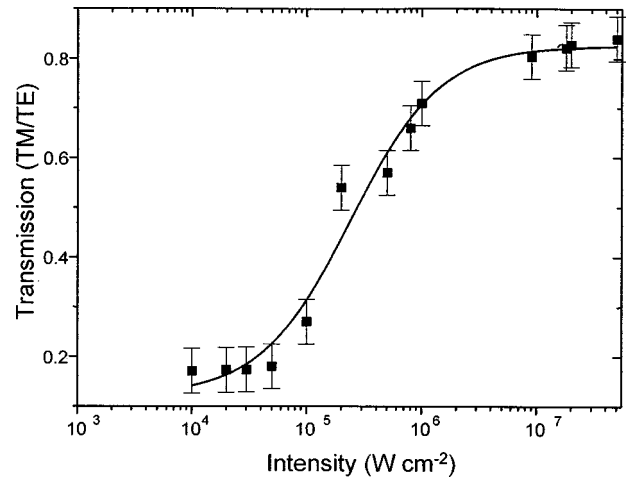


FIG. 2. Transmission for TM polarized light as a function of beam intensity.

$$\alpha(I) = \frac{\alpha_0}{1 + I/I_s}, \quad (2)$$

where  $I_s$  is the saturation intensity given by

$$I_s = \frac{n_r}{2\mu c} \frac{(E_{\text{ISB}} - \hbar\omega)^2 + \hbar/\tau_{\text{ISB}}\hbar\gamma}{M_{12}^2}, \quad (3)$$

where  $E_{\text{ISB}} = E_2 - E_1$ ,  $n_r$  is the refractive index.

Transmission as a function of the intensity is reported in Fig. 2. By fitting experimental data, a saturation intensity of  $1.7 \text{ MW/cm}^2$  was obtained. Assuming  $E_{\text{ISB}} = 0.68 \text{ meV}$  and using the calculated  $M_{12}$ , we can estimate from Eq. (3) an ISB relaxation time  $\tau_{\text{ISB}}$  of about  $9 \pm 3 \text{ ps}$ .

Differential transmission as a function of the delay time between pump and probe is reported in Fig. 3. Pump-induced probe transmission at a given time delay  $\tau$  changes according to the relation:<sup>18</sup>

$$\Delta T(\tau) \propto \int_{-\infty}^{+\infty} I(t - \tau) \Delta n(t) dt, \quad (4)$$

where  $I(t)$  is the probe intensity,  $\Delta n(t) = n_1(t) - n_2(t)$ ,  $n_1$  and  $n_2$  being electron density in the C1 and C2 conduction band, respectively. Since the typical pulse duration is less than 120 fs, the differential transmission simply relates to  $n_1(\tau) - n_2(\tau)$ . Differential transmission and hence popula-

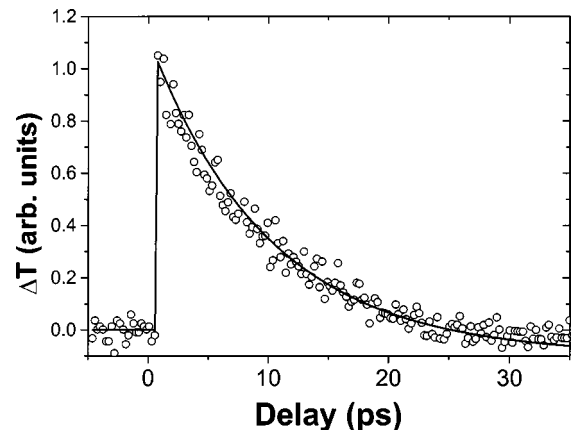


FIG. 3. Time-resolved differential transmission for a probe beam at 680 meV. Full line is the single-exponential fit.

tion in the excited state C2 decay is less than 20 ps. Assuming a single-exponential decay, a time constant of the order of 10.5 ps is obtained. This value is within the limits estimated from saturation intensity measurements.

From the measured transmission transient, some insight about relaxation processes can be attempted. In the case of ISB transitions at wavelength in the 5–10  $\mu\text{m}$  range, reported relaxation times are of the order of 1–2 ps.<sup>19</sup> Asano *et al.* observed an ISB relaxation time of 2.7 ps for a transition at 500 meV.<sup>14</sup> They proposed that the longer relaxation time is due to the contribution related to intrasubband relaxation. The overall ISB relaxation time is given by the equation:  $\tau = \tau_{\text{ISB}} + E_{\text{ISB}}/\hbar\omega_{\text{LO}}\tau_{\text{in}}$ , where  $\tau_{\text{ISB}}$  and  $\tau_{\text{in}}$  are the intersubband and the intrasubband relaxation times,  $\hbar\omega_{\text{LO}}$  the AlAs interface mode phonon energy (47 meV). In the present case assuming an ISB energy of 680 meV, one would obtain an overall relaxation time of 3.4 ps, lower than the value experimentally measured. As remarked above, the system InGaAs/AlAs in the case of narrow wells exhibits strong coupling between  $\Gamma$ -like states of the well and  $X$ -like states of the barrier. After excitation to the C2 level, relaxation to  $X$  valley and subsequent acoustic phonon-assisted relaxation to the C1 state is a process competitive to direct  $\Gamma$ – $\Gamma$  decay (see Fig. 1). To check the presence of different relaxation channels, multiexponential fitting was performed. Best fitting was obtained with two decay constants of 6.5 and 65 ps, which may support the proposed picture of a fast ( $\Gamma$ – $\Gamma$ ) and slow ( $\Gamma$ – $X$ ) relaxation channel, although the fast time constant is larger than that obtained from the theoretical estimate given above. Relative weights for the fast and slow constants are 78% and 22%, respectively. This suggests that fast direct  $\Gamma$ – $\Gamma$  decay is the predominant relaxation process. Since  $\Gamma$ – $X$  relaxation depends on the overlap integral between  $\Gamma$  and  $X$  states,<sup>20</sup> we can conclude that C1 and C2 conduction-band states have a strong  $\Gamma$  character. This is confirmed by the good agreement between our calculated transition matrix elements and those obtained by tight-binding calculation for the same structure.

In conclusion, we measured transmission and intersubband relaxation time in InGaAs/AlAs multiple quantum wells with a large transition energy (680 meV) by means of pump and probe experiments. The differential transmission

decay is of the order of 10 ps, which suggests that  $\Gamma$ – $\Gamma$  relaxation is the predominant mechanisms for ISB relaxation. These results are promising to exploit the advantages of a fast ISB relaxation in the near-infrared region around 1550 nm. With the material system investigated in the present work, this could be obtained by coupled asymmetric quantum wells.

The authors wish to acknowledge A. Barberis, F. Beltram, and A. Franciosi for help and discussions.

- <sup>1</sup>See J. Faist, F. Capasso, D. Sivco, C. Sirtori, A. L. Hutchinson, S. N. G. Chu, and A. Y. Cho, *Science* **264**, 553 (1994).
- <sup>2</sup>B. F. Levine, R. J. Malik, J. Walker, K. K. Choi, C. G. Bethea, D. A. Kleinman, and M. Vanderberg, *Appl. Phys. Lett.* **50**, 273 (1987).
- <sup>3</sup>S. D. Frohlich, R. Wille, W. Schlapp, and G. Weimann, *Phys. Rev. Lett.* **50**, 1749 (1987).
- <sup>4</sup>A. Seilmeier, H. J. Hubner, G. Abstreiter, G. Weinman, and W. Schlapp, *Phys. Rev. Lett.* **59**, 1345 (1987).
- <sup>5</sup>F. H. Julien, J. M. Lourtioz, N. Herschkorn, D. Delacourt, J. Pocholle, M. Papuchon, R. Planel, and G. LeRoux, *Appl. Phys. Lett.* **53**, 116 (1988).
- <sup>6</sup>T. Elsaesser, R. J. Bauerle, W. Kaiser, H. Lobentanzer, W. Stolz, and K. Ploog, *Appl. Phys. Lett.* **45**, 256 (1989).
- <sup>7</sup>D. Y. Oberle, D. R. Wake, M. V. Klein, J. Klem, T. Henderson, and H. Morkoç, *Phys. Rev. Lett.* **59**, 696 (1987).
- <sup>8</sup>J. H. Smet, L. H. Peng, Y. Hirayama, and C. G. Fonstad, *Appl. Phys. Lett.* **64**, 986 (1994).
- <sup>9</sup>T. Asano, S. Noda, T. Abe, and A. Sasaki, *Proceedings of Photonics in Switching*, Sendai, 1995, p. 153.
- <sup>10</sup>T. Asano, S. Noda, T. Abe, and A. Sasaki, *J. Appl. Phys.* **82**, 3385 (1997).
- <sup>11</sup>J. M. Jancu, V. Pellegrini, R. Colombelli, F. Beltram, B. Mueller, L. Sorba, and A. Franciosi, *Appl. Phys. Lett.* **73**, 2621 (1998).
- <sup>12</sup>P. Dawson, K. J. Moore, C. T. Foxon, G. W. Hooft, and R. P. M. Van Hal, *J. Appl. Phys.* **65**, 3606 (1989).
- <sup>13</sup>R. Teissier, J. J. Finley, M. S. Skolnick, J. W. Cokburn, J. L. Pelouard, R. Grey, G. Hill, M. A. Pate, and R. Planel, *Phys. Rev. B* **54**, R8329 (1996).
- <sup>14</sup>T. Asano, S. Noda, and K. Tomoda, *Appl. Phys. Lett.* **74**, 1418 (1999).
- <sup>15</sup>J. J. Shi and E. Goldys, *IEEE Trans. Electron Devices* **46**, 83 (1999).
- <sup>16</sup>*Landolt-Bornstein: Numerical Data and Functional Relationship in Science and Technology*, edited by O. Madelung, Group III, Vol. 17a (Springer, Berlin, 1982) and Vol. 22a (Springer, Berlin, 1987).
- <sup>17</sup>S. Pan and S. Feng, *Phys. Rev. B* **44**, 8165 (1991).
- <sup>18</sup>W. Heiss, E. Gornik, H. Hertle, B. Murdin, G. M. H. Knippels, C. J. G. Langerak, F. Schaffler, and C. R. Pidgeon, *Appl. Phys. Lett.* **66**, 3313 (1995).
- <sup>19</sup>S. Lutgen, R. A. Kaindl, M. Woerner, T. Elsaesser, A. Hase, and H. Kunzel, *Phys. Rev. B* **54**, R17343 (1996).
- <sup>20</sup>J. Feldmann, J. Nunnenkamp, G. Peter, E. Gobel, J. Kuhl, K. Ploog, P. Dawson, and C. T. Foxon, *Phys. Rev. B* **42**, 5809 (1990).